The Astronomical Journal, 149:164 (8pp), 2015 May doi:10.1088/0004-6256/149/5/164

A COMPREHENSIVE PHOTOMETRIC STUDY OF THE CONTACT BINARY GN BOO WITH POSSIBLE MAGNETIC ACTIVITIES

J. J. Wang[1,2,3], S. B. Qian[1,2,3], Y. P. Zhang[4], J. Zhang[1,2,3], J. J. He[1,2,3], E. G. Zhao[1,2,3], L. Y. Zhu[1,2,3], W. P. Liao[1,2,3], and L. Liu[1,2,3]
[1] National Astronomical Observatories/Yunnan Observatories, Chinese Academy of Sciences, P.O. Box 110, 650216 Kunming, China; wjjbxw@ynao.ac.cn
[2] Key Laboratory for the Structure and Evolution of Celestial Objects, Chinese Academy of Sciences, 650216 Kunming, China
[3] Graduate School of the Chinese Academy of Sciences, Yuquan Road 19, Shijingshan Block, 100049 Beijing, China
[4] Department of Astronomy, Beijing Normal University, 100875 Beijing, China
Received 2015 January 6; accepted 2015 March 17; published 2015 April 23

ABSTRACT

Multi-color photometric data of GN Boo observed from 2010 to 2013 are presented. The intrinsic variations of the light curves are remarkable, and their phenomena are probable evidence of stronger magnetic activities on the surfaces of the components. Based on all CCD times of minimum light, a secular increase superimposed on a cyclic oscillation is found. The orbital period increases at a rate of $dP/dt = +1.74 \times 10^{-7}$ days yr^{-1}, which can be explained by mass transfer from the less massive component to the more massive one. The period and amplitude of the cyclic variation are $P = 9.5632$ yr and $A = 0.0046$ days, respectively, which correspond to the previous published results. Using the 2010 version of the W–D code, five sets of photometric solutions were derived from our new data. The results imply that the stellar spot, the degree of fill-out, and the temperature difference ΔT between the components of GN Boo are variable. It is inferred that the magnetic activities perhaps influence the outer radius of the component, causing the temperature of the component star and the level of contact to change.

Key words: binaries: close – stars: activity – stars: evolution – stars: individual (GN Boo)

1. INTRODUCTION

Many additional studies on stellar spots are presented by Li et al. (2014), Liu et al. (2012), Qian et al. (2012, 2014), Yang et al. (2013b), Wang et al. (2014), Zhang et al. (2014a, 2014b), and Samec et al. (2015) based on the distortions of the light curves in close binaries. Holzwarth & Schüssler (2002) pointed out that the starspot preferred longitudes can be explained by tidal effects on the dynamics of magnetic flux tubes, which are thought to give rise to starspots as they emerge on the stellar surface. The variations in the spot radius may be caused by starspot evolution (Zhang et al. 2014b). From observations with the Chinese Small Telescope ARray in Antractica, Qian et al. (2014) obtained that the lifetime of a dark spot is close to 116 days. The components in W UMa-type binaries share a common convective envelope (CCE), which lies between the inner and outer critical Roche-lobe surfaces. In general, their light curves are typical EW types, where there is a very small difference in light variability between the depths of the two minima. However, the light curves of many contact systems whose corresponding magnetic activities have been investigated, such as EQ Tau (Li et al. 2014), CW Cas (Wang et al. 2014), and DZ Psc (Yang et al. 2013b), are variable. Unfortunately, the properties of magnetic activities and CCE are not well understood. Do the magnetic activities have an effect on CCE or stellar evolution of the component? In order to have a better understanding, it is necessary to monitor late-type stars using multi-color photometry and spectroscopy.

GN Boo (=GSC 2022-0079) was discovered by the Robotic Optical Transient Search Experiment (ROTSE-I) from the all-sky surveys for variable stars (Akerlof et al. 2000). Blattler & Diethelm (2001) presented a new ephemeris of MinI = 2451996.4139+0.301601 × E, which was derived from their one light curve without a filter. About 750 observations in the VR_c band had been obtained by Sanders et al. (2005), whose curves with total eclipses were used to determine its period of 0.3016027 days. They also concluded that GN Boo is a W-type contact binary with a mass ratio of $q = 0.33$, a fill-out of $f = 21\%$, a temperature difference of $\Delta T = 360$ K between the two components, and a dark spot on the more massive component. Later, Yang et al. (2013a) pointed out that the O'Connell effect in previously published data might disappear in their symmetric light curves, and that GN Boo is a marginal-contact binary with the overcontact degree of $f = 5.8 \pm 0.1\%$. The cyclic variations in the O–C diagram are probably attributed to the magnetic activity or light-time effect of the third body.

To investigate the variations in the light curve and orbital period for GN Boo, we have monitored it for four consecutive years. From our observations, the distortions in the light curves are remarkable, especially in the depth at eclipse. Our new light curves are analyzed using the Wilson–Devinney code, version 2010. Finally, we discuss the magnetic activities and CCE in detail.

2. OBSERVATIONS

Photometric observations of GN Boo were carried out from 2010 April to 2013 May with the 85 and 60 cm telescopes at the XingLong station (XLs) of the National Astronomical Observatories of the Chinese Academy of Sciences, and the 60 cm telescope at the Yunnan Observatories (YNO). These telescopes were equipped with the standard Johnson–Cousin–Bessel BVR_cI_c filters. All CCD observed images were reduced with aperture photometry of the DAOPHOT package in IRAF. The coordinates of the comparison star (C) and the check star (CH) are listed in Table 1. The mean photometric error for individual observations is less than 0.01 mag.

With the linear ephemeris equation (Yang et al. 2013a),

$$\text{Min. I (HJD)} = 2451996.4156 + 0^{\text{d}}.30160220 \times E, \quad (1)$$

Table 1
Coordinates of the Contact Binary GN Boo (V), the Comparison Star (C), and the Check Star (CH)

Stars	α_{2000}	δ_{2000}	V_{mag}
GN Boo (V)	$14^h50^m07\overset{s}{.}8$	$+29°38'58\overset{''}{.}5$	11.12
SDSSJ145007+293949 (C)	$14^h50^m07\overset{s}{.}6$	$+29°39'49\overset{''}{.}8$	15.41
TYC 2022-0167 (CH)	$14^h50^m08\overset{s}{.}1$	$+29°36'02\overset{''}{.}8$	13.96

the light curves along with phase and differential magnitude were obtained. Five sets of curves in the VR_c band are displayed in Figure 1, which reveals that the light curves on 2010 April 23 and May 20 belong to typical EW types (e.g., the depths of the two minima are almost equal). However, the depth of the primary eclipse has been obviously different from that of the secondary eclipse since 2011. The obvious O'Connell effect was found from the observations on 2011 May 5. Meanwhile, we also carried out BVR_cI_c-band observations for the first time with the 85 cm telescope on 2012 April 15, May 25, and June 4 and 2013 February 26, March 15, and March 21, respectively. The complete multi-color light curves are plotted in Figure 2.

As shown in Figures 1 and 2, the depth difference between the primary eclipse and the secondary one increased with time. Using a parabolic fitting method, we calculated the differential magnitudes at extreme light, and these magnitudes are listed in Table 2. The heights of maximum light are unequal on 2010 May 20 and 2011 May 5, which proves the presence of the O'Connell effect. Combined with the R_c-band light curve taken from Yang et al. (2013a), we compared these light curves of GN Boo in Figure 3, where the differential magnitudes at the primary were adjusted to be −1.25 mag. In the left panel of Figure 3, the variations occur before the secondary eclipse, whereas the outlines after that are stable. Our light curves observed in 2013 are similar to those in 2012, but the shapes of the light curves in 2012 and 2013 are different from previous observations (2010 and 2011). These phenomena are likely to be evidence of stronger magnetic activities on the surface of at least one component.

From those CCD photometric data, several times of minimum light were determined with a parabolic fitting method. All of the eclipse times are listed in Table 3.

3. THE ORBITAL PERIOD VARIATIONS OF GN BOO

After GN Boo was discovered by Akerlof et al. (2000), some investigators published the photoelectric and CCD eclipse times. Sanders et al. (2005) suggested that its orbital period may be decreasing. Yang et al. (2013a) compiled 17 photoelectric and 45 CCD minimum light times to reveal a cyclic period change ($A_3 = 0.0042$ days, $P_3 = 9.89$ yr) superimposed on a linear increase. In this section, we re-analyze the orbital period changes with all CCD times of minimum light (Tables 3 and 4, and the data from Yang et al. 2013a).

The O–C values are plotted in the upper panel of Figure 4 with the ephemeris Equation (1) given by Yang et al. (2013a), where only a continuous increase (dashed line) cannot describe the trend of the O–C very well. With the same weight, a nonlinear least-squares fitting yields the following ephemeris,

$$\begin{aligned}\text{Min. I (HJD)} = {} & 2451996.4170(6) + 0\overset{d}{.}3016012(3) \times E \\ & + 7.19(1.8) \times 10^{-11} \times E^2 + A_3 \\ & \times \left[\frac{1 - e^2}{1 + e\cos\nu} \sin(\nu + \omega) + e \sin\omega \right], \quad (2)\end{aligned}$$

which implies that the orbital period variations include a secular increase and a cyclic oscillation. The quadratic term in Equation (2) suggests that the period of GN Boo may increase at a rate of $dP/dt = +1.74(44) \times 10^{-7}$ days yr^{-1}. The cyclic oscillation of the orbital period mostly results from the light-time travel effect of a third body (Liao & Qian 2010). The parameters of the third body are taken from Irwin (1952), and are determined as the periodic amplitude $A_3 = 0.0046$ (± 0.0002) days, the period $P_3 = 9.5632(\pm 0.1511)$ yr, the eccentricity $e = 0.24$, the time of periastron $T = 2451679.5484$ (± 198.1456), and the longitude of periastron $\omega = 259\overset{\circ}{.}2291$ (± 21.8852) for GN Boo. The overall trend of a cyclic variation and continuous increase is shown with a solid line in the upper panel of Figure 4. The solid line in the middle panel represents the oscillation with an amplitude of 0.0046 days and a period of 9.5632 yr, which are close to the results given by Yang et al. (2013a). The corresponding residuals with respect to Equation (2) are graphed in the bottom panel of Figure 4. Similar period changes have been found in some contact binaries, such as ER Cep (Liu et al. 2011), FU Dra (Liu et al. 2012), AA UMa (Lee et al. 2011), and DZ Psc (Yang et al. 2013b). Therefore, these kinds of period variations for GN Boo may be reliable.

4. PHOTOMETRIC SOLUTIONS WITH THE W–D PROGRAM

The photometric solutions were derived using the Wilson–Devinney program, version 2010 (Wilson & Devinney 1971; Wilson 1979, 1990, 2008; van Hamme & Wilson 2007). This new version does not input limb-darkening coefficients by band. When we choose logarithmic functions (ld = −3), the program itself can automatically calculate them using subroutine LIMDARK, which is based on the limb-darkening tables calculated using the method of van Hamme (1993).

Before calculating the solutions, we should obtain the temperature of GN Boo. Sanders et al. (2005) assumed the effective temperature of the primary star to be 5750 K. Yang et al. (2013a) proposed the spectral type of this system to be G8V, and the corresponding temperature is 6250 K. However, according to Allen's Astrophysical Quantities (Cox 2000), the temperature of a star with G8 spectra in the main sequence is determined to be 5310 K, which is lower than that given by previous authors. To confirm its spectral type, low-resolution spectra were obtained using the 2.16 m telescope at the XLs of the National Astronomical Observatory on 2012 May 14. The spectroscopic data were reduced with standard packages in IRAF. By comparing the spectra of GN Boo (black line) with that of a G8V standard star (red line) from the Stellar Spectral Flux Library (Pickles 1998) in Figure 5, we can see that they are similar. Thus, the spectral type of GN Boo is G8V, and the corresponding effective temperature of the primary

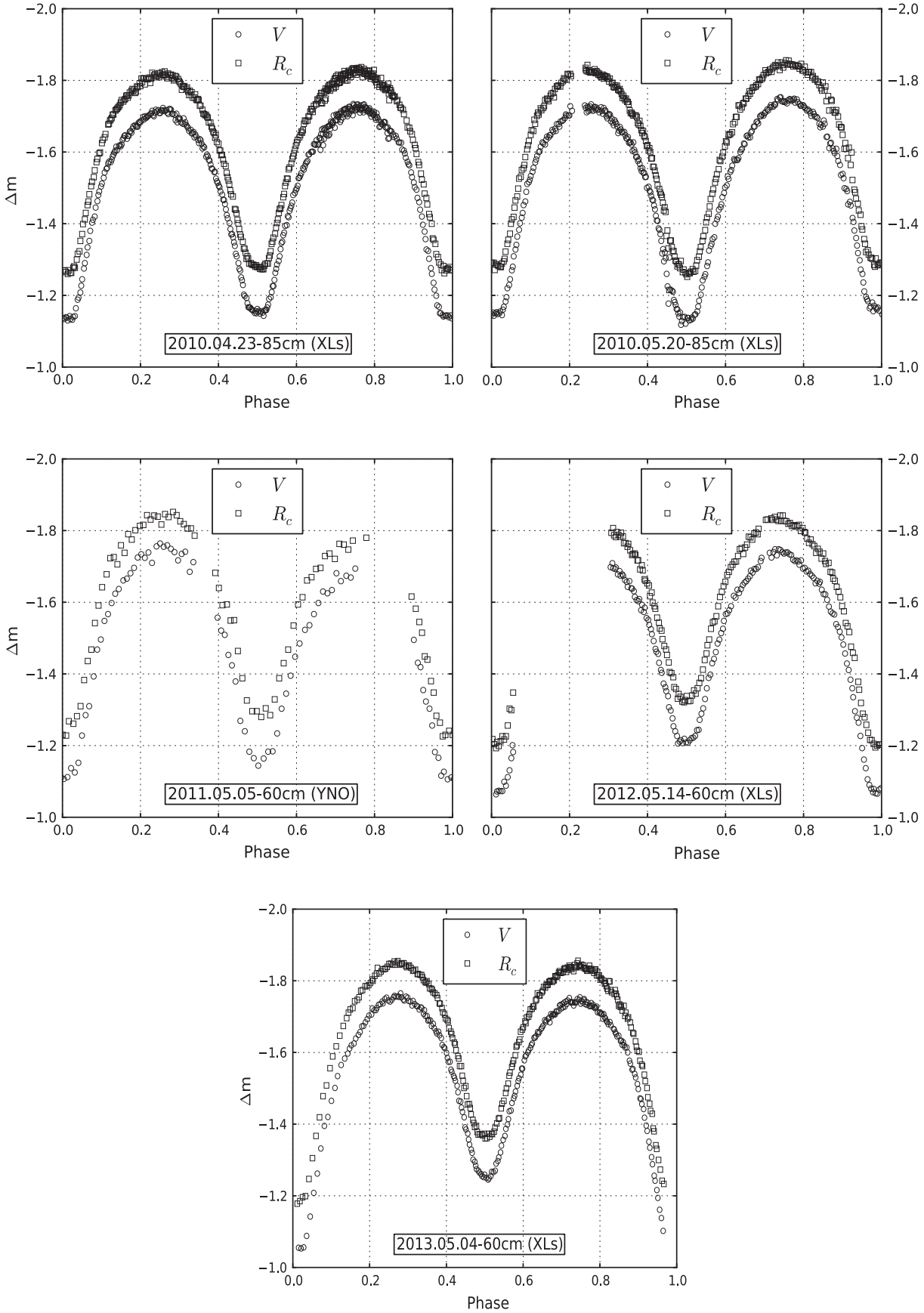

Figure 1. VR_c-band light curves of GN Boo observed from 2010 to 2013.

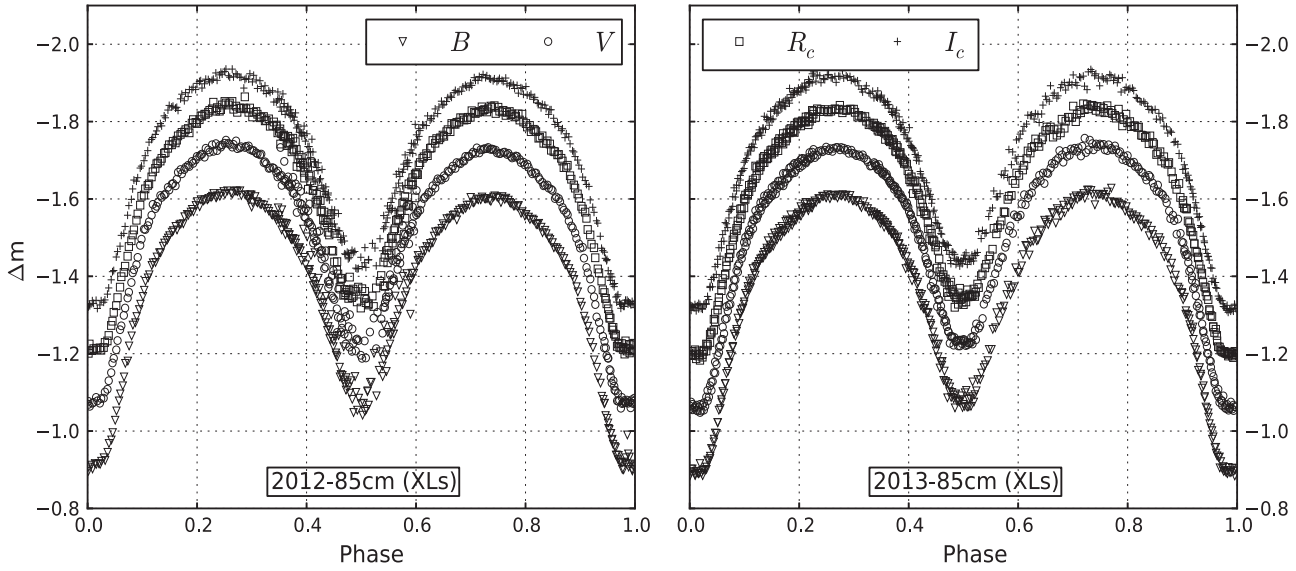

Figure 2. BVR_cI_c-band light curves of GN Boo observed in 2012 and 2013.

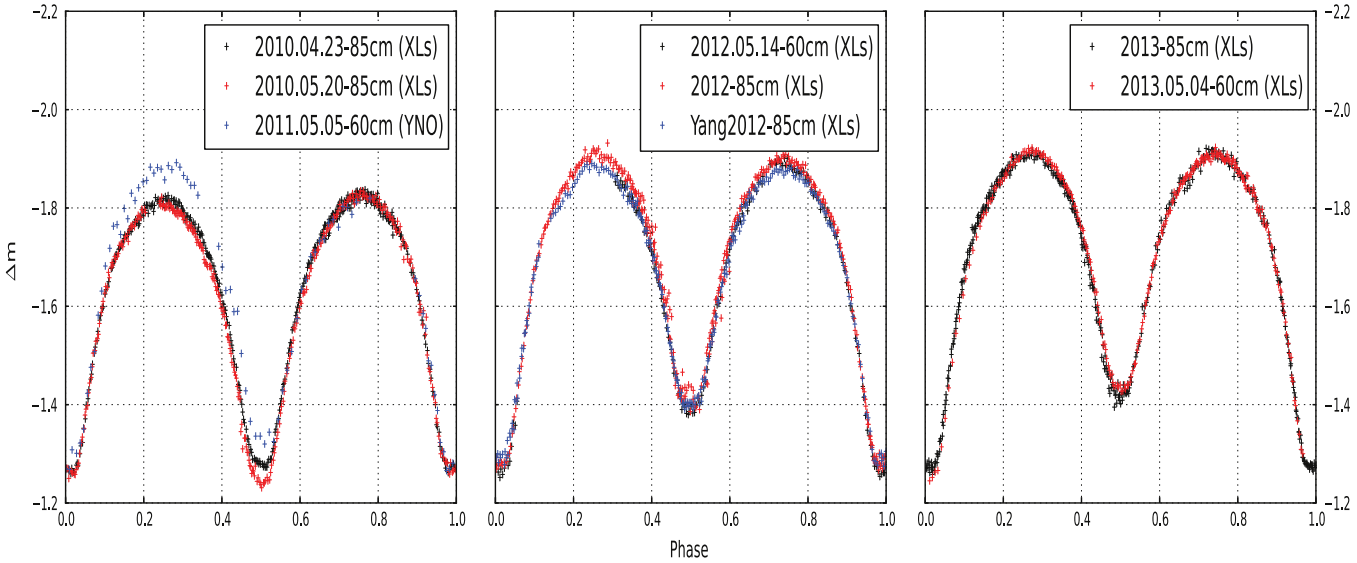

Figure 3. Comparison of the R_c-band light curves for GN Boo. Yang (2012) data are taken from Yang et al. (2013a).

Table 2
Differential Magnitude Values in R_c-band Light Curves at Two Maxima and Two Minima for GN Boo

Date	MinI (mag)	MinII (mag)	MaxI (mag)	MaxII (mag)	MinI–MinII (mag)	MaxI–MaxII (mag)	MinI–MaxII (mag)
2010 Apr 23	−1.25	−1.27	−1.82	−1.82	0.02	0.00	0.57
2010 May 20	−1.28	−1.26	−1.83	−1.85	−0.02	0.02	0.57
2011 May 05	−1.23	−1.30	−1.84	−1.78	0.07	−0.06	0.55
2012	−1.21	−1.34	−1.84	−1.84	0.13	0.00	0.63
2013	−1.20	−1.36	−1.83	−1.83	0.16	0.00	0.63

component is adopted as $T_1 = 5310$ K (Cox 2000). Assumed convective outer envelopes for both components, the bolometric albedo coefficients $A_1 = A_2 = 0.5$ (Ruciński 1969) and the values of the gravity-darkening coefficients $g_1 = g_2 = 0.32$ (Lucy 1967) are used.

Yang et al. (2013a) confirmed that GN Boo is a W-type contact binary. Based on our BVR_cI_c-band data observed in 2013, the solutions are obtained for a series of mass ratios ($q = 1.0 \sim 5.0$). The corresponding mass ratio q versus the squared residuals Σ are plotted in Figure 6, which is in

Table 3
CCD Times of Minimum Light with Different Telescopes from 2010 to 2013

Date	Telescope	Min.	JD (Hel.)	Error (days)
2010 Apr 23	XLs-85 cm	I	2455310.11136	0.00019
2010 Apr 23	XLs-85 cm	II	2455310.26242	0.00009
2010 May 19	XLs-85 cm	II	2455336.20069	0.00008
2010 May 20	XLs-85 cm	II	2455337.10514	0.00016
2010 May 20	XLs-85 cm	I	2455337.25609	0.00015
2011 May 05	YNO-60 cm	I	2455687.11880	0.00024
2011 May 05	YNO-60 cm	II	2455687.27255	0.00033
2012 Feb 14	YNO-60 cm	II	2455972.28726	0.00031
2012 Feb 14	YNO-60 cm	I	2455972.43725	0.00017
2012 May 14	XLs-60 cm	II	2456062.16530	0.00012
2012 May 14	XLs-60 cm	I	2456062.31639	0.00028
2012 May 25	XLs-85 cm	I	2456073.17445	0.00021
2012 Jun 04	XLs-85 cm	II	2456083.27825	0.00040
2013 Jan 22	YNO-60 cm	I	2456315.36323	0.00014
2013 Jan 25	YNO-60 cm	I	2456318.37907	0.00019
2013 Feb 26	XLs-85 cm	II	2456350.19814	0.00019
2013 Feb 26	XLs-85 cm	I	2456350.34930	0.00016
2013 Mar 21	XLs-85 cm	I	2456373.27134	0.00011
2013 May 04	XLs-60 cm	II	2456417.15486	0.00010

Table 4
Some CCD Times of Minimum Light

JD (Hel.)	Error (days)	References	JD (Hel.)	Error (days)	References
2452500.0916	0.0007	(1)	2456009.5366	0.0010	(3)
2454994.0352	…	(2)	2456057.4903	0.0020	(4)
2454994.1841	…	(2)	2456058.3956	0.0015	(4)
2455280.8580	…	(2)	2456062.4670	0.0018	(4)
2455621.5223	…	(2)	2456066.3881	0.0020	(4)
2455622.5764	…	(2)	2456066.5390	0.0022	(4)
2455968.6682	…	(2)	2456398.7575	0.0003	(5)
2455993.5503	…	(2)	2456408.5605	0.0013	(6)
2456009.3847	0.0027	(3)	…	…	…

References. (1) Kreiner (2004), (2) *O–C* gateway, (3) Hubscher et al. (2013), (4) Martignoni (2014), (5) Nelson (2014), (6) Hubscher (2013).

accordance with the q–Σ diagram in VR_c given by Yang et al. (2013a). Therefore, the photometric mass ratio is reliable, and a suitable mass ratio for GN Boo is $q \sim 3.5$.

In Figure 3, our R_c-band light curve observed with the 60 cm telescope is similar to that with the 85 cm telescope in 2012 and 2013. All of our light curves are divided into five groups, which were obtained on 2010 April 23, 2010 May 20, and 2011 May 05 and in 2012 and 2013, respectively. Meanwhile, late-type components exhibit much stronger magnetic activity because of deep convection and fast rotation. Sanders et al. (2005) obtained a dark spot on the more massive component of GN Boo. As shown in Figure 3, the variations and asymmetries of light curves are possibly due to stellar spots on the surfaces of the components, and so we employed spots in our modeling. Five sets of photometric solutions with spots are listed in Table 5, where the parameters of the spots hint that the stellar spot on the primary component varies with time. The theoretical light curves (solid lines) from the Light Curve program (LC) of the Wilson–Devinney code are plotted in Figure 7.

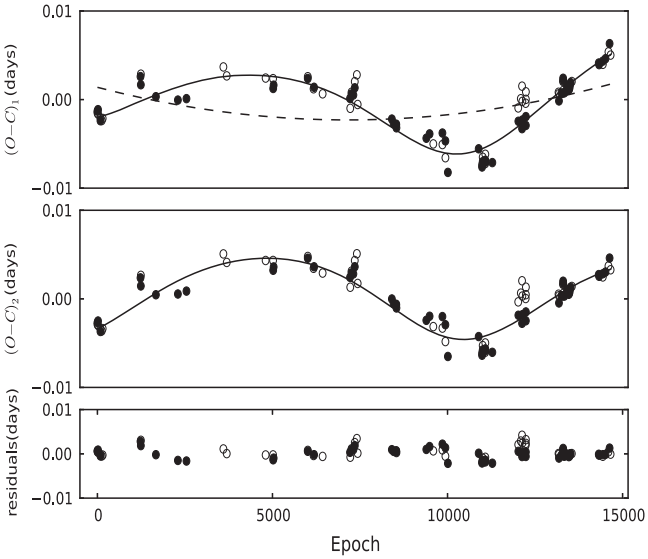

Figure 4. *O–C* diagram for GN Boo. The filled circles represent the times of the primary eclipse, the open circles refer to the secondary ones.

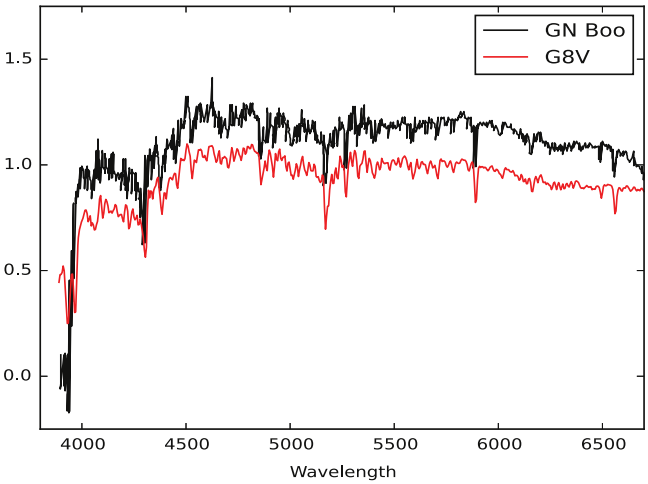

Figure 5. Low-resolution spectra of GN Boo obtained with the 2.16 m telescope on 2012 May 14. The red line shows the spectra of a G8V standard star given by Pickles (1998), and the black shows those for GN Boo.

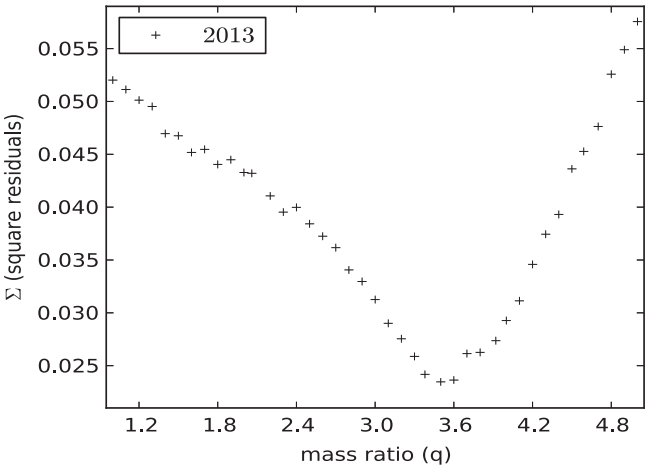

Figure 6. Mass ratio q vs. squared residuals Σ for GN Boo derived with BVR_cI_c-band light curves in 2013.

Table 5
Photometric Solutions with Spots and Third Light for GN Boo in Different Observational Seasons

	2010 Apr 23	2010 May 20	2011 May 05	2012	2013
$i(^\circ)$	82.26 ± 0.21	84.87 ± 0.23	83.71 ± 1.020	84.90 ± 0.19	84.44 ± 0.27
T_1(K)	5310	5310	5310	5310	5310
T_2(K)	5180 ± 6	5253 ± 6	5068 ± 14	4864 ± 6	4860 ± 3
$\Omega_1 = \Omega_2$	6.6775 ± 0.0050	6.6424 ± 0.0060	6.6261 ± 0.0223	6.7050 ± 0.0072	6.7115 ± 0.0112
q (M_2/M_1)	3.14057(fixed)	3.14057(fixed)	3.14057(fixed)	3.14057(fixed)	3.14057 ± 0.00750
$L_{1B}/(L_{1B} + L_{2B})$	…	…	…	0.4050 ± 0.0022	0.4063 ± 0.0018
$L_{1V}/(L_{1V} + L_{2V})$	0.2920 ± 0.0012	0.2774 ± 0.0013	0.3208 ± 0.0039	0.3728 ± 0.0015	0.3738 ± 0.0013
$L_{1R_c}/(L_{1R_c} + L_{2R_c})$	0.2870 ± 0.0011	0.2753 ± 0.0011	0.3107 ± 0.0032	0.3512 ± 0.0013	0.3519 ± 0.0011
$L_{1I_c}/(L_{1I_c} + L_{2I_c})$	…	…	…	0.3370 ± 0.0013	0.3376 ± 0.0011
$L_{3B}/(L_{1B} + L_{2B} + L_{3B})$	…	…	…	0.0827 ± 0.0107	0.0794 ± 0.0083
$L_{3V}/(L_{1V} + L_{2V} + L_{3V})$	0.0056 ± 0.0026	…	…	0.0365 ± 0.0064	0.0443 ± 0.0057
$L_{3R_c}/(L_{1R_c} + L_{2R_c} + L_{3R_c})$	0.0034 ± 0.0020	…	…	0.0209 ± 0.0047	0.0312 ± 0.0046
$L_{3I_c}/(L_{1R_c} + L_{2I_c} + L_{3R_c})$	…	…	…	0.0304 ± 0.0060	0.0342 ± 0.0050
$\theta(^\circ)$	124.39	124.39	90.00	90.00	90.00
$\phi(^\circ)$	8.15	5.73	92.29	28.66	210.38
$r_{\rm spot}(^\circ)$	24.36	21.50	30.10	14.33	8.05
T_s/T_*	1.275	1.375	0.700	0.700	1.225
$f = (\Omega - \Omega_{\rm in})/(\Omega_{\rm in} - \Omega_{\rm out})$	$20.00 \pm 0.80\%$	$25.66 \pm 0.96\%$	$28.29 \pm 3.6\%$	$15.57 \pm 1.16\%$	$14.53 \pm 1.80\%$
Σres^2	0.004354	0.005392	0.002894	0.019774	0.018480

5. DISCUSSIONS AND CONCLUSIONS

The O–C diagram of GN Boo shows its orbital period changes as a secular increase superimposed on a cyclic oscillation. The quadratic trend of the O–C_1 reveals that the orbital period is increasing continuously at a rate of $dP/dt = +1.74(44) \times 10^{-7}$ days yr^{-1}. With the following well-known equation,

$$\dot{P}/P = 3\dot{M}_1\left(1/M_2 - 1/M_1\right), \quad (3)$$

the mass transfer from the less massive component to the more massive one is estimated as $dM_1/dt = -0.76 \times 10^{-7}\, M_\odot$ yr^{-1}. The timescale of mass transfer for the less massive star is $\tau_1 \sim M_1/\dot{M}_1 \sim 3.6 \times 10^6$ yr, which is close to its thermal timescale of $GM_1{}^2/R_1L = 4.1 \times 10^6$ yr. Thermal mass transfer from the less massive component to the more massive one can explain the secular increase of the orbital period. The cyclic oscillation ($A_3 = 0.0046$ days, $P_3 = 9.5632$ yr) is close to that reported by Yang et al. (2013a). Based on their discussions, it may arise from the light-time effect of the third body or the magnetic activities of the components.

In order to understand the variations in the light curves, five sets of the adjustable parameters (i, T, Ω, q, L, l_3, and spots) were derived using the Wilson–Devinney program. Depending on these solutions, we discuss the nature of the variations in two main aspects.

5.1. Extrinsic Variability of Binary System

The extrinsic variability of close binaries results from purely geometrical effects (rotation, orbital motion, and an additional body), whereas the brightness of the component itself is constant. In the photometric solutions, the extrinsic parameters listed in Table 5 are the inclination i and third light l_3. The inclination on 2010 April 23 was 82°.26, less than the others. Does the variable inclination cause the variations in the light curves? To find out, we plot all R_c-band differential magnitudes at extreme light in Figure 8. It is seen that the depth at primary eclipse varies non-monotonically with that at secondary eclipse. When the primary eclipses become brighter, the secondary ones will be fainter. However, the orbital inclination should result in a synchronous increase or decrease in the global luminosity. On the other hand, the third light, like the orbital inclination, can decrease the brightness of both eclipse simultaneously because the addition of a constant to a positive function diminishes its "fractional" or "percent" variation (Kallrath & Milone 2009).

Therefore, the inclinations and third light are not enough to cause the distortions in the light curves from 2010 to 2013.

5.2. Intrinsic Activities of the Component

The light curves of some contact binaries, e.g., AD Cnc (Qian et al. 2007), CK Boo (Yang et al. 2012), DZ Psc (Yang et al. 2013b), EQ Tau (Li et al. 2014), and CW Cas (Wang et al. 2014), are variable on timescales of years, months, or days. These phenomena are evidence of starspot activities of the components. Sanders et al. (2005) modeled his asymmetric light curves and obtained a dark spot on the more massive component of GN Boo. In Table 5, we can see that the location, radius, and temperature of the spot on the surface of the primary component change with time, and the stellar spots are only on the less massive one. It is inferred that the variations in the light curves of GN Boo are due to stellar spot activities. To explore the relations between the magnetic activity (stellar spot) and evolution of contact binaries, some information (differential magnitudes Δm, temperature difference ΔT, and degree of fill-out f) is included in Table 6. The temperature difference is 629 K (Yang et al. 2013a) and the degree of fill-out is only 5.8%, while the difference is 57 K in 2010 and the corresponding contact is 25.7%. It is suggested that the contact with greater ΔT will be at the lowest fill-out, which agrees with the statistical relation between the fill-out and the temperature difference presented by Samec et al. (2011). The variable degree of the fill-out in such a short time implies that it would evolve with a dynamic timescale.

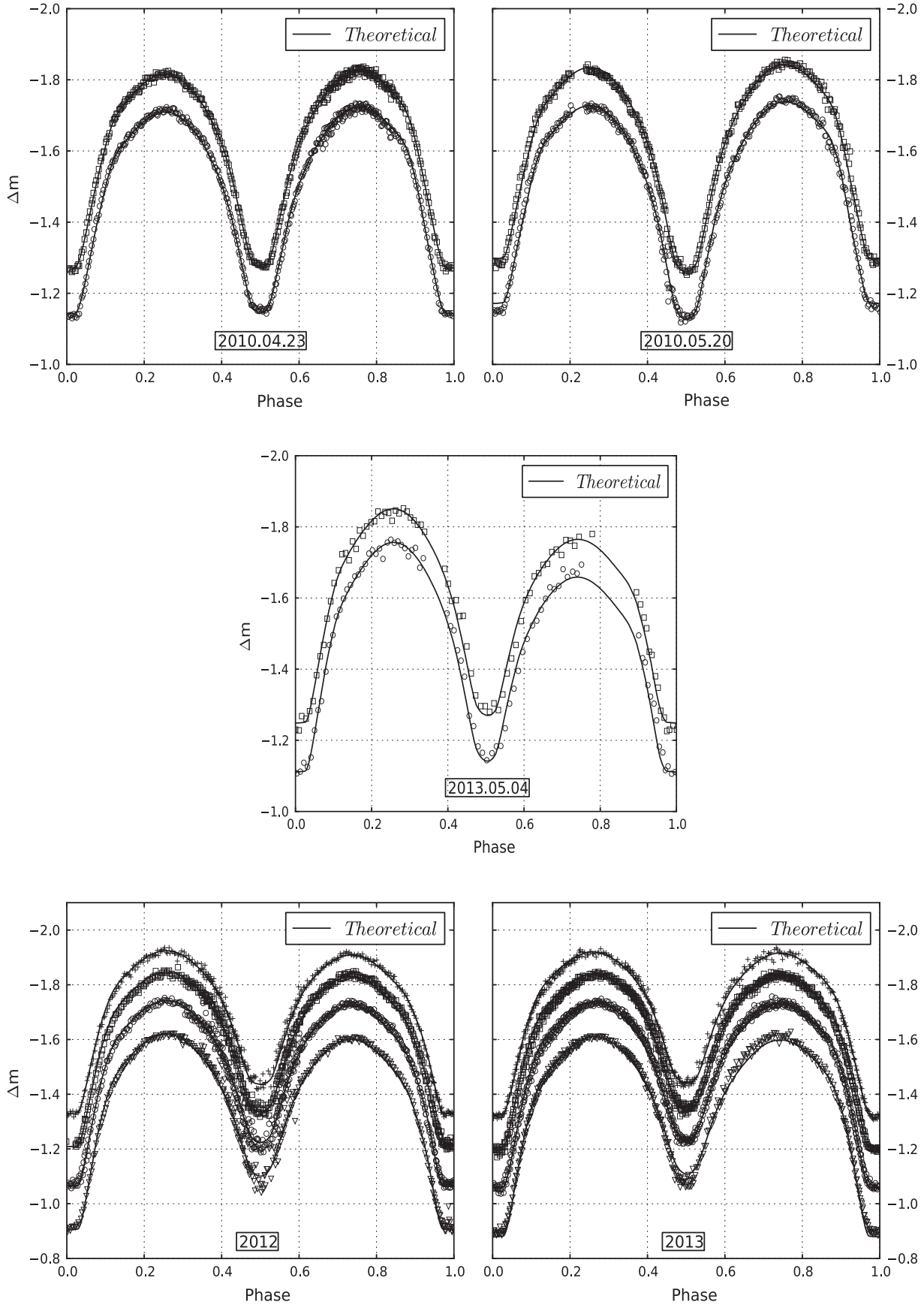

Figure 7. Five sets of theoretical light curves. Our light curves in 2012 and 2013 contain observations with the 60 and 85 cm telescopes at XingLong station.

Table 6
Differential Magnitude of Extreme Light in R_c-band Light Curves, the Temperature Difference between the Components, and the Degree of Fill-out at Different Times

Date	MinI–MinII (mag)	MaxI–MaxII (mag)	$\Delta T(T_1 - T_2)$ (K)	Degree of Fill-out (%)	References
2005 Mar	...	...	360	21	Sanders et al. (2005)
2010 Apr 23	0.02	0.00	130 ± 6	20.0 ± 0.8	Present work
2010 May 20	–0.02	0.02	57 ± 7	25.7 ± 1.0	Present work
2011 May 05	0.07	–0.06	242 ± 24	28.3 ± 3.6	Present work
2012 Mar 04	0.11	0.00	629 ± 10	5.8 ± 0.1	Yang et al. (2013a)
2012	0.13	0.00	446 ± 3	15.6 ± 1.2	Present work
2013	0.16	0.00	450 ± 5	14.5 ± 1.8	Present work

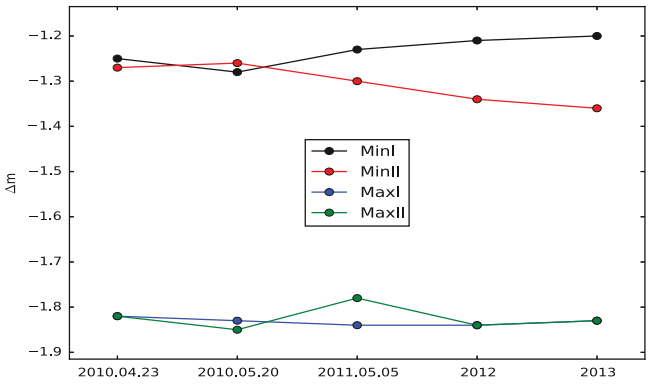

Figure 8. Comparison of the R_c-band differential magnitudes at extreme light.

As we know, the thermal timescale of the components is in megayears, and the star evolving by itself cannot lead to such large temperature variations in such a short time. However, contact binaries have an extremely physical environment, e.g., fast rotation and CCE, which make stellar evolution of the component different from the signal star. Yakut & Eggleton (2005) suggested that the rotational shear is almost certainly the main driver of magnetic activity in cool stars with convection zones. The outer 10% by radius could change its structure much more rapidly, since its mass and thermal energy are much smaller than that overall. Li et al. (2004) inferred that W-subtype contact binaries may be caused by expansion of the primary or by contraction of the secondary. If the magnetic activities efficiently restrain energy from transporting in the convective zone, the outer radius will increase. It is possible that the magnetic activity has influence on the outer structure of the component, and its variable radius may cause the temperature of component star and the CCE to change. Chabrier et al. (2007) also pointed out that the fast rotation and/or magnetic activity may significantly affect the evolution of eclipsing binaries from their evolutionary calculations using a phenomenological approach. Similar results are found in the other contact binaries, e.g., EQ Tau (Li et al. 2014) and V404 And (Zhang et al. 2014a). Therefore, magnetic activities, e.g., CCE, may play an important role in the evolution of contact binaries.

GN Boo is a good target to understand magnetic activity and binary evolution, but it is still necessary to obtain photometric and spectroscopic observations to check the nature of the intrinsic variations.

This work is supported by the Chinese Natural Science Foundation (Nos. 11203066 and 11325315), the Science Foundation of Yunnan Province (2012HC011), the Strategic Priority Research Program "The Emergence of Cosmological Structures" of the Chinese Academy of Sciences, grant No. XDB09010202, and the Key Laboratory Foundation of the Chinese Academy of Sciences. We are indebted to our supervisor and many observers.

REFERENCES

Akerlof, C., Amrose, S., Balsano, R., et al. 2000, AJ, 119, 1901
Blattler, E., & Diethelm, R. 2001, IBVS, 5125, 1
Chabrier, G., Gallardo, J., & Baraffe, I. 2007, A&A, 472, 17
Cox, A. N. 2000, Allen's Astrophysical Quantities (New York: Springer), 389
Holzwarth, V., & Schüssler, M. 2002, AN, 323, 399
Hubscher, J. 2013, IBVS, 6084, 1
Hubscher, J., Braune, W., & Lehmann, P. B. 2013, IBVS, 6048, 1
Irwin, J. B. 1952, ApJ, 116, 211
Kallrath, J., & Milone, E. F. 2009, Eclipsing Binary Stars: Modeling and Analysis (Berlin: Springer)
Kreiner, J. M. 2004, AcA, 54, 207
Lee, J. W., Lee, C.-U., Kim, S.-L., Kim, H.-I., & Park, J.-H. 2011, PASP, 123, 34
Li, L. F., Han, Z. W., & Zhang, F. H. 2004, MNRAS, 355, 1383
Li, K., Qian, S. B., Hu, S. M., & He, J. J. 2014, AJ, 147, 98
Liao, W. P., & Qian, S. B. 2010, MNRAS, 405, 1930
Lucy, L. B. 1967, ZA, 65, 89
Liu, L., Qian, S.-B., Zhu, L.-Y., et al. 2011, MNRAS, 415, 3006
Liu, L., Qian, S.-B., He, J.-J., et al. 2012, PASJ, 64, 48
Martignoni, M. 2014, IBVS, 6091, 1
Nelson, R. H. 2014, IBVS, 6092, 1
Pickles, A. J. 1998, PASP, 110, 863
Qian, S. B., Yuan, J. Z., & Soonthornthum, B. 2007, ApJ, 671, 811
Qian, S.-B., Zhang, J., Zhu, L.-Y., et al. 2012, MNRAS, 423, 3646
Qian, S.-B., Wang, J.-J., Zhu, L.-Y., et al. 2014, ApJS, 212, 4
Ruciński, S. M. 1969, AcA, 19, 245
Samec, R. G., Labadorf, C. M., Hawkins, N. C., Faulkner, D. R., & van Hamme, W. 2011, AJ, 142, 117
Samec, R. G., Koenke, S. S., & Faulkner, D. R. 2015, AJ, 149, 30
Sanders, S. J., Bradsteet, D. H., & Hargis, J. R. 2005, AAS, 37, 1478
van Hamme, W. 1993, AJ, 106, 2096
van Hamme, W., & Wilson, R. E. 2007, ApJ, 661, 1129
Wang, J. J., Qian, S. B., He, J. J., Li, L. J., & Zhao, E. G. 2014, AJ, 148, 95
Wilson, R. E. 1979, ApJ, 234, 1054
Wilson, R. E. 1990, ApJ, 356, 613
Wilson, R. E. 2008, ApJ, 672, 575
Wilson, R. E., & Devinney, E. J. 1971, ApJ, 166, 605
Yakut, K., & Eggleton, P. P. 2005, ApJ, 629, 1055
Yang, Y. G., Qian, S. B., & Dai, H. F. 2013a, AJ, 145, 60
Yang, Y. G., Qian, S. B., Zhu, L. Y., Dai, H. F., & Soonthornthum, B. 2013b, AJ, 146, 35
Yang, Y. G., Qian, S. B., & Soonthornthum, B. 2012, AJ, 143, 122
Zhang, L. Y., Yang, Y. G., Pi, Q. F., & Zhu, Z. Z. 2014a, AJ, 147, 66
Zhang, L. Y., Pi, Q. F., & Yang, Y. G. 2014b, MNRAS, 442, 2620